Deutscher Wetterdienst

Annalen der Meteorologie

36

Vorhersage: Wetter, Klima, Umwelt

Symposium zur Einhundertfünfzigjahrfeier des Preußischen Meteorologischen Instituts 16. und 17. Oktober 1997 in Berlin

Offenbach am Main 1998

Selbstverlag des Deutschen Wetterdienstes

Zur Herstellung dieses Buches wurde chlor- und säurefreies Papier verwendet.

ISSN 0072-4122
ISBN 3-88148-339-X

Herausgeber und Verlag:

Deutscher Wetterdienst
Frankfurter Straße 135
63067 Offenbach am Main

INHALT

The hydrological cycle in present and future climate

Lennart Bengtsson
Max Planck Institute for Meteorology
Bundesstr. 55, D-20146 Hamburg

Abstract

The present study reports some recent modelling investigations of the hydrological cycle. Considerable progress has taken place in the reconstruction of the hydrological cycle with the help of advanced numerical models. In an area like the Baltic Sea and its catchment region it appears possible to reproduce the hydrological cycle with considerable accuracy. A global reconstruction of the hydrological cycle is also making progress and ways have been found to avoid the problems with spin-off effects in the data-assimilation. Validation issues are severe and must be addressed more vigorously including a better understanding of the three-dimensional net radiative forcing.

The natural variability of precipitation on longer time scales has been studied in relation to the water balance of the catchment area of the Caspian Sea. Preliminary studies indicate that models may be able to simulate the observed multi-decadal variability, but more experiments are needed to demonstrate any potential predictability. Present coupled models have nevertheless reached a state of sophistication where such experiments are becoming feasible.

The possible change of the hydrological cycle in a future climate is still difficult to predict. Model experiments with increased greenhouse gases only show an overall increase, in particular over land and at high latitudes, specially in winter. When the effect from aerosols is considered the answer is less clear and as is shown in this paper can even lead to an overall weakening of the hydrological cycle.

1. Introduction

Despite the fundamental importance of water for society, we have insufficient knowledge of the different components of the hydrological cycle; precipitation, evapo-transpiration, storage of water in lakes and aquifers and river run-off. Even more difficult is it to determine how the hydrological cycle may change in a future climate with an altered concentration of greenhouse gases, ozone and aerosols caused by anthropogenic influences. Major scientific efforts are now being devoted to increasing our knowledge in this important field. This research is being undertaken over a broad area, incorporating major observational programmes and different indirect ways to estimate the hydrological cycle with the help of advanced numerical models. In this paper we are mainly concerned with this indirect approach and we will present and discuss some recent results from calculations by numerical models.

Precipitation has a very fine, almost fractal scale, and is virtually impossible to sample from the standard synoptic stations (Bergeron, 1970). Measurements are almost exclusively confined to the populated land areas of the earth. For the ocean areas conventional precipitation data are

missing. Data from island stations exist but are usually not representative for the ocean surface due to orographic and land-sea effects, except perhaps of some small atolls and low level islands. Many efforts have been undertaken to create estimates of the climatological distribution of precipitation, in recent decades for example by Jaeger (1976) and Legates and Willmott (1990). Both these data sets have significant weaknesses and should in no way be considered as the truth. The Legates and Willmott climatology gives a global mean precipitation which is some 15% higher than the one from Jaeger, the reason being that the precipitation estimates are based on differently assumed net radiative forcing at the surface of the earth. Over ocean areas the "climatologies" are at best crude estimates.

Under the auspices of the GEWEX programme, major efforts are being undertaken to improve our empirical knowledge of precipitation and other components of the hydrological cycle. A global precipitation climatology project (GPCP) has been set up to provide improved precipitation data (Rudolf et al., 1996). These data sets are based on space (2.5° lat/lon) - and time (monthly) -averaged data including high resolution in-situ observations and different satellite estimates. A compiled data set now exists for the 10-year period 1986-1996.

One of the satellite estimates is obtained from the geostationary satellites by relating the outgoing long wave radiation (OLR) from cloud top pixels, in the band 10.5-12.5 μm at temperatures lower than 235 K, to the intensity of convective rainfall. (Arkin and Meisner, 1987, Janowiak and Arkin, 1991). This method is rather inexact and is furthermore only applicable in the tropics. Special difficulties exist to separate tropical cirrus anvils and high ice clouds at higher latitudes.

Another satellite estimate is to make use of the Special Sensor Microwave Imager (SSM/I) on the polar orbiting satellites. Radiances are measured at four frequencies near 19, 22, 37 and 85 GHz, respectively. At these frequencies it is possible to detect the effect of hydrometeors on radiative transfer (Grody, 1991 and Weng and Grody, 1994). Measurements are only possible over water since land surface emissivity are rather similar to water clouds. Serious problems exist in using SSM/I data for estimating precipitation. One such limitation is sampling problems in combination with the high time variability of precipitation. Jung et al. (1998) have carried through evaluation of precipitation for the area of the Baltic Sea indicating a clear underestimation compared to calculations from high resolution numerical models. Fig. 1 shows the precipitation from August 1987 from GPCP (only in-situ observation), OLR and SSM/I. The differences between the different data sets are considerable.

Observation of evapotranspiration are virtually non-existent except at a few experimental sites and water exchange with groundwater is similarly insufficiently known. Data for river run-off have been systematically collected, in some regions for more than 100 years, and the river run-off from the larger rivers is reasonably well measured. One key aspect of the GEWEX program is de facto to use well monitored river basins and lakes as an independent way of estimating the water balance. In section three, we will present some results from the Baltex program where a combination of models and data have been used to determine the water cycle in the Baltic Sea region. Finally, the percolation of water through the ground and the movement and residence time of water underground is only poorly known.

We summarize also in Fig. 2 two different estimates of the global hydrological cycle, one by Baumgartner and Reichel (1975) and another by Chahine (1992). The figure shows separately precipitation and evaporation over land and ocean, the net transport of water vapour from the ocean to land and the return river flow. It is interesting to note that the hydrological cycle over

land consists to 2/3 of recirculated water. Accumulation of snow on glaciers is estimated according to (Bromwich, 1990). This water will in due course return to the ocean through calving of icebergs but generally on a much longer time scale.

2. The hydrological cycle and the energy balance of the atmosphere

The heat balance of the atmosphere and the redistribution of solar radiation is one of the central questions for our understanding of the climate system. The solar irradiance, according to the best available measurements, amounts to 341 Wm^{-2} (1/4 of the solar constant), of which slightly more than 30% is reflected back to space due to reflections from clouds, from the surface of the earth and from back-scattering by the air and dust particles in the air (planetary albedo). Of the remaining 240 Wm^{-2}, some 146 Wm^{-2} reach the surface while the remaining part is absorbed in the atmosphere. While we can be confident in the amount of incoming and reflected solar radiation, since it can be well measured by satellite sensors, the same accuracy does not hold for the amount which reaches the surface. In fact, the amount, which is absorbed in the atmosphere according to the latest ground measurements, Ohmura and Gilgen (1993) some 25 Wm^{-2} higher then previously assumed. The possible causes to this large absorption is still being disputed and may be further revised (Ramanathan et al., 1995).

The same amount of heat, 240 Wm^{-2}, which enters the earth returns to space in the form of terrestrial radiation. However, that takes place in a somewhat complex way since the surface is cooled (and the atmosphere correspondingly heated) by both surface radiative emission and fluxes of sensible and latent heat. The atmosphere in return is radiating back to the surface (due to water vapour and other greenhouse gases) and the net surface radiation amounts to some 45 Wm^{-2}, an amount which at best is known with an accuracy of some 10%. The sensible heat flux from the surface is 14-20 Wm^{-2} and the latent heat flux is estimated to be as high as 80-88 Wm^{-2}, which is more than 1/3 of net incoming solar radiation, Fig. 3.

It follows from the global heat balance in Fig. 3 that the inaccuracies in the atmospheric absorption of short and long wave radiation, which may be as high as 10-15 Wm^{-2}, also means that the sum of the sensible and latent heat, in order to close the surface heat balance, will suffer the same inaccuracy. If this inaccuracy is distributed proportionally between sensible and latent heat it follows that the global averaged evaporation and precipitation is probably only known with an accuracy of some 15% or by 150 mm equivalent precipitation/year.

This analysis also highlights the problem of estimating precipitation by numerical modelling, since on an average the evaporation must balance the radiation imbalance at the ground. If that is wrong so will the water balance be. The relatively good agreements in the estimates of the water cycle shown in Fig. 2 are simply due to the fact that the assumed net radiative forcing used in the two studies apparently were rather similar.

3. Model reconstruction of the hydrological cycle

From the discussion in the previous section, it is clear that over a suitable period of time the amount of precipitation must balance that of evaporation from the surface, and hence, from the numbers in Fig. 3, the annual global precipitation should be equal to about 1000 mm/year. Now for a limited area and for a limited time we must know the net transport of moisture through the boundaries as well as the net exchange of water with the ground. However, due to the difficulties to estimate the divergent wind component from wind observations, this direct approach can only be considered in areas with accurate and homogenous radiosondes. It is particularly diffi-

cult in regions with strong transient quasi-geostrophic flow, where the divergent part of the wind is significantly smaller than the rotational part of the wind and where furthermore the divergent wind undergoes rapid changes in time and space. The approach in recent studies has instead been to rely on advanced atmospheric models where the divergent wind is calculated from the model equations as constrained by available observations. For a recent discussion of this approach reference is made to Trenberth (1997). The numerical prediction models are now using more advanced methods for flux calculations than present bulk formulas used in empirical studies, so one could not really use the simple empirical expressions to seriously question the model calculations.

High resolution modelling under the BALTEX programme has quite successfully predicted precipitation in the catchment area of the Baltic Sea as validated against high density precipitation measurements, but with a tendency to a slight overprediction (Bengtsson et al., 1998). In these modelling experiments limited high resolution models have been successively updated at the boundaries by analyzed data sets from meteorological services. Table 1 shows predicted and measured results for the period August-October 1995 calculated by the German REMO model (Jacob and Podzun, 1997).

Total monthly mean precipitation		
mm/month	modeled	measured
August 95	56.2	56.7
September 95	88.4	75.5
October 95	48.0	40.6

Table 1: Predicted and measured precipitation for September 1995 for the Baltic Sea drainage area. The very high resolution precipitation data have been collected under the auspices of the BALTEX programme. The predicted precipitation has been obtained by the REMO model (Jacob et al., 1997) at 1/6° resolution. The REMO model has been forced at the boundaries by analysed data (every 6 hours) from the German meteorological service. The attached table gives the results for each month August-October 1995.

A remaining issue, not yet satisfactorily solved, is the so called spin-up effect. The numerical models are usually initialized through a data-assimilation procedure whereby an estimate (first guess) of the actual initial state is provided by a short range prediction from a previous initial state some 6 to 12 hours earlier. The first guess is then being modified by the new observations and the analysis increment is added to the first guess. This new state is not any longer in balance with the model equations because of the observed increment. The imbalance will be dissipated away as gravity waves after some time ranging from hours to several days, but in the meantime the model contains noise which significantly can disturb the three-dimensional divergence and associated fluxes. The new initial state must therefore be initialized in order at least to assure a balance between the wind- and the massfield. The balance with respect to physical processes cannot be achieved as easily and therefore available numerical weather prediction schemes suffer from being improperly adjusted. This create difficulties to properly balance energy- and moisture fluxes. To minimize the "spin-up" problem one can calculate the energy- and water balance from the ensemble of first guess estimates, mostly consisting of 6-hrs forecast fields. This is generally too short to efficiently eliminate non-meteorological features, and as can be

seen from different studies (Bengtsson,1995 and Jeuken et al., 1996) it takes several days to reduce the noise and achieve an acceptable balance. In the re-analyses, recently carried out at ECMWF (Gibson et al., 1997), ensembles of 6- and 24-hrs forecasts have been made available. As can be seen from Fig. 4, showing the global hydrological cycle in the same way as Fig. 2, the errors in the water balance are as large as the total continental run-off, making these data sets less useful for studies of the water cycle. Over limited areas there are even an overall negative water balance over some major river basins.

However, when the models are integrated further in time an energy- and water balance is gradually achieved. The disadvantage is then that systematic model errors start to accumulate, thus gradually changing the hydrological cycle. Furthermore forecasts ensembles with a length of several days are normally not available. In order to combine the balance of physical processes of the climate model with an observed sequence of observable atmospheric states and hence be able to better undertake model validation, we have carried through an experiment of successive adjustment or "nudging" towards a sequence of large scale analyses of vorticity, divergence, temperature and surface pressure (Krishnamurti et al., 1991, Jeuken et al., 1996).

By doing so, we can gradually adjust the climate model towards the observed state of the real atmosphere, while still maintaining the full dynamical and physical interactions of the climate model to generate its own internally consistent evolution of physical processes. The overall principle is outlined in Fig. 5. The adjustment is being done by means of a forcing term for the large scale motion only, which is added to the actual equations. The timescale for the adjustment term is of the same order as the timescale for geostrophic adjustment. The largest weights in the adjustment is put on the surface pressure and relative vorticity with smaller weights on temperature and the divergent part of the wind. The moisture field is *not* used at all and no data is used in the surface boundary layer. The principal idea behind the design of the experiments was to maintain enough freedom for the climate model to develop internally consistent fluxes while only being constrained by the large scale atmospheric flow. The design of the numerical experiment is outlined in Fig. 6.

The analyzed fields for every 6 hours from the operational ECMWF data base (T213, 31 levels, envelope orography) was first interpolated to the resolution of the ECHAM model (T106, 19 levels, mean orography) for the period January - March 1993. A simulation with the ECHAM model was then carried out using the SST data for same period but gradually adjusting the climate model to the interpolated analyzed fields from the ECMWF model as indicated in Fig. 6.

Fig. 7 shows the sea level pressure and model-simulated clouds for a sequence (every 6 hrs.) of adjusted ECHAM fields for 25 March 1993. The sea level pressure data are practically identical to the original data from ECMWF for this resolution (not shown). The model-generated clouds are synoptically realistic and agree quite well with observed cloud patterns. The result shows that the moisture field, both as water vapour and cloud liquid water, can be generated from the three-dimensional atmospheric circulation given realistic boundary conditions for land and sea. Fig. 8 shows the globally averaged water balance for the year 1993. In this case the experiment was analogue to the one above but instead we used a model run at T42 resolution in order to better compare with the climate simulation. As can see from the figure the nudging approach can provide an overall satisfactory global water balance. A similar good balance is obtainable for atmospheric energy, which is also out of balance in the numerical analyses including the ECMWF re-analyses (Stendel and Arpe, 1997).

There are some fundamentally important conclusions to draw from this experiment. The first is that the hydrological cycle is more or less fully controlled by atmospheric dynamics. Areas of convergence and divergence determine where precipitation will occur, and surface wind, temperature and vertical lapse rate determine the intensity of evaporation. Over land the key issue is to determine the potential evapo-transpiration, that is to know the amount of soil moisture and the efficiency of vegetation in releasing water vapour.

A series of numerical studies presently being undertaken within the BALTEX numerical experimentation programme have highlighted the importance of initializing soil moisture. In the catchment area of the Baltic Sea, the spin-up time of soil moisture is of the order of one to a few months. Storage of water in the ground needs to be determined more accurately for the prediction of river run-off. Another important finding, which I believe could be generalized, is that models with prescribed SST in the Baltic Sea generally tend to overpredict evaporation due to the lack of SST adjustment to atmospheric temperature. This temperature adjustment can be quite rapid in situations with strong winds and strongly stratified ocean basins. Coupled ocean/atmosphere models (Hagedorn, 1998) are certainly required to handle air-sea interaction processes in a satisfactory way.

4. Possible changes in the water cycle

Precipitation in the Sahel region has undergone large scale changes, from dry conditions in the early part of this century to wetter conditions in the 1950s and thereafter becoming dryer again. Superimposed on this multi-decadal fluctuations are shorter variations of a few years´ duration.

I will here report of another such low-frequency phenomenon which has received considerable interest in recent years, namely the variation of the water level of the Caspian Sea. The Caspian Sea is the biggest lake on earth and covers an area of some 0.37 milj. km^2. The total drainage area is 3.1 milj. km^2, with 86% of the run-off coming from Volga and the Ural river. The Caspian Sea has no run-off so the inflow of water from rivers and precipitation over the lake must be balanced by evaporation. During the period 1933-1977 the water level fell with 2.9 m, and the size of the lake shrank by some 6%, having disastrous economic and environmental consequences in the area (Rodionov, 1994). It was thought by many that the drying out of the lake had anthropogenic causes, but after 1977 the water level started to rise and had by the end of 1996 more or less recovered the water losses from the previous period, (Golitsyn, 1995). However, the economical and environmental consequences were equally severe.

Studies have now demonstrated that the variation in the water level is strongly correlated with the Volga river run-off. The Volga drainage basin is specifically exposed to precipitation patterns associated with typical decadal to multi-decadal fluctuations in the general circulation. Northerly cyclone tracks generate higher then normal precipitation in the Volga drainage basin, while southerly cyclone tracks favour dryer conditions. The interesting scientific questions are now whether climate models are able to simulate the typical low-frequency variations in the storm tracks and the associated variations in precipitation, river run-off and fluctuations in the lake water level, and additionally to answer the question what the main reason is for these changes. The final and most important question, namely whether the water level can be predicted, must await a satisfactory outcome of the first two questions.

The Max Planck Institute for Meteorology in Hamburg has in cooperation with scientists from the Russian republic and Kazakhstan been trying to answer these questions (Arpe et al., 1998). In the experiments carried out, the global sea surface temperatures from the beginning of this

century were prescribed and used to drive an atmospheric model through the whole of this century. The result can be seen in Fig. 9 which shows the predicted and observed river run-off into the Caspian Sea from Volga. The units are given in cm/year of the average water level, where one cm is equivalent to 3.7 km^3/year. It appears that the large scale variations in the river run-off is reasonably well reproduced by the model. In another experiment we modified the tropical sea surface temperatures by removing all interannual variations. At middle and high latitudes the temperatures were unchanged. In this case we were not able to reproduce the observed evolution, which suggests that tropical sea surface temperature may be responsible for the observed variations. Needless to say, more experiments are required to clarify this, but it appears that the findings make physical sense, since the tropical forcing of the atmosphere is much more steady and robust than the forcing from the oceans at higher latitudes. It may also be that the result is fortuitous and is due to stochastic forcing of individual meteorological events giving rise to the observed low frequency response. However, other experiments presently being carried out suggest a genuine predictability. Future investigations will certainly clarify this better.

5. The water cycle in a future climate

We will restrict the discussion in this section to a preliminary analysis of a series of climate change experiments recently completed at the Max Planck Institute in Hamburg (Roeckner et al., 1998). The experiments consider the effects of greenhouse gases, sulfate aerosols and tropospheric ozone, Table 2. The experiments have been carried out with a coupled atmosphere-ocean model (Roeckner et al., 1996) which have been integrated from 1860 until 2050 using observed greenhouse gases until 1990 and thereafter an assumed increase according to established scenarios by IPCC (IS92a with recent updates for CFCs).

Name	Forcing due to changing atmospheric concentrations of ...	Years
GHG	CO_2 and other well mixed greenhouse gases	1860 - 2100
GSD	GHG plus sulfate aerosols (direct effect only)	1860 - 2050
GSDIO	GHG plus sulfate aerosols (direct and indirect effect) plus tropospheric ozone	1860 - 2050
CTL	Unforced control experiment	300

Table 2: List of experiments.

In GHG the concentration of the following greenhouse gases is prescribed as a function of time: CO_2, CH_4, N_2O and a large number of individual industrial gases including CFCs, hydrochlorofluorocarbon, hydrofluorocarbons, carbon tetrachloride and metylchloroform. Each gas has been treated separately.

In GSD, the greenhouse gases are treated as in GHG, but with the added effect of anthropogenic emission of sulfur in the troposphere. Global emission from fossil fuel burning and from other industrial emissions increases from approximately 10 million ton sulfur (MtS) in 1900 to about 75 MtS in 1995, growing further according to IS92a to 150 MtS in 2050. In the experiment GSD

we have incorporated a rather comprehensive treatment of the sulfur cycle, including conversion from SO_2 to SO_4, atmospheric 3D-transport and wet and dry deposition of sulfate. In the experiment GSD, only the direct effect of scattering in clear air is included.

The GSDIO experiment differs from GSD in two respects. Firstly, we have incorporated the indirect aerosol effect on cloud albedo and secondly we have allowed the tropospheric ozone distribution to change as a result of the prescribed anthropogenic emission of precursor gases.

The global temperature increases in all three experiments as can be seen from Fig. 10, with a marked warming becoming noticeable from the 1980s onward. The observed surface temperature is indicated as a comparison. The largest warming is obtained in the GHG experiment and the smallest in the GSDIO. Comparison with equilibrium calculations with an ocean mixed layer model, Table 3, suggests that the transient integrations in a global average have a similar response to the forcing from greenhouse gases, tropospheric ozone and aerosols as in the equilibrium integrations, except the time delay of some 40 years caused by the thermal inertia of the ocean. The temperature increase is largest at high latitudes but as can be seen from Fig. 11, this is also where the compensating cooling from the aerosol-effect is largest.

Exp. No.	Historical forcing experiments (1860 - -> 1990)	Radiative Forcing [Wm^{-2}]	Temp. Response [°C]	Climate Sensitivity [$°C/Wm^{-2}$]
1	Well mixed greenhouse gases (CO_2, CH_4, N_2O, CFC's)	2.12	1.82	0.86
	* IPCC value from 1750 to 1994	(2.45)*		
2	Tropospheric ozone	0.37 (0.2 to 0.6)	0.34	0.91
3	Direct sulfate aerosol	- 0.34 (-0.2 to -0.8)	- 0.24	0.71
4	Indirect sulfate aerosol	- 0.89 (0 to -1.5)	- 0.78	0.87
5	Effects (1 to 4) included	1.26	1.13	0.90

Table 3: Global annual mean radiative forcing at the top of the tropopause and equilibrium response in global annual mean surface air temperature

What is then the change of the hydrological cycle in a future climate? Based on some genera reasoning (Ramanathan, 1998), if there is no change in the solar absorption but only an increase in the net downward radiation (because of the greenhouse gases), the respond will be increased surface fluxes of latent and sensible heat. The warmer surface (dominated by the oceans) will evaporate more moisture which in turn will increase the global precipitation. The increased atmospheric temperature at the same time, according to Clausius-Clapeyron´s equation, will be able to hold more moisture. In fact, most numerical calculations suggest that the relative humidity is almost conserved, since the dynamical processes which regulate the mixing of water va-

pour in the atmosphere hardly change at all. Approximately, therefore, one degree warming of the atmosphere will increase moisture by some 6%. Water vapour is therefore probably the strongest feedback factor in the atmosphere, roughly leading to a doubling of the original forcing from the anthropogenic greenhouse gases.

However, a more detailed calculation suggest that the increased moisture in the atmosphere must also effect the solar forcing due to enhanced scattering as well as absorption of solar radiation in the atmosphere. Table 4 summarizes the surface heat balance for the three experiments: GHG, GSD and GSDIO compared with the control experiment at the time of the anticipated doubling of the anthropogenic greenhouse gases in the 2040s. The latent heat flux increases compared to the control for GHG and GSD but diminishes for GSDIO. The reason is enhanced atmospheric absorption of solar radiation combined with a negative short wave cloud forcing. There is in fact in the GSDIO experiment a negative surface heat flux, so the warming at the surface (+1.41°C) is partly due to the reduced surface cooling by the smaller latent heat flux!

Surface fluxes	CTL [W/m^2]	GHG-CTL [W/m^2]	GSD-CTL [W/m^2]	GSDIO-CTL [W/m^2]
Sensible heat	- 11.9	+ 0.65	+ 0.82	+ 0.78
Latent heat	- 81.9	- 1.30	- 0.35	+ 0.47
Shortwave radiation	+ 148.8	- 3.29	- 4.19	- 5.33
Longwave radiation	- 52.7	+ 5.35	+ 4.98	+ 5.09
Surface air temperature [°C]	14.69	+ 2.34	+ 1.82	+ 1.41
Precipitation (P) or evaporation (E)	2.82 [mm/d]	+ 1.5 [% of CTL]	+ 0.4 [% of CTL]	- 0.6 [% of CTL]
P (continents)	2.13 [mm/d]	+ 7.5 [% of CTL]	+ 5.0 [% of CTL]	+ 2.5 [% of CTL]
E-P (oceans)	0.30 [mm/d]	+ 14.1 [% of CTL]	+ 11.1 [% of CTL]	+ 5.4 [% of CTL]

Table 4: Change of global annual mean surface heat fluxes and other climate variables in scenario experiments (decade 2040 to 2050) minus control experiment CTL (150-y mean). Sign convention: downward fluxes positive, upward fluxes negative.

The hydrological cycle is enhanced over land in all experiments, most so in the GHG. Precipitation is everywhere reduced over oceans, most so in GSDIO when also evaporation is weakened. The general difference between land and ocean is presumably due to an enhanced monsoon effect caused by the relatively larger warming over land areas. Snow accumulation increases for all experiments due to higher temperatures over Antarctica and Greenland. The increased accumulation is largest for GSD but goes down again for GSDIO due to the reduced hydrological cycle.

The regional change in the hydrological cycle is difficult to estimate due to internal chaotic processes of different time scales. Fig. 12 shows the same as Fig. 11 but for precipitation. The pre-

cipitation in the ITCZ increases in all experiments and most so in experiment GHG. There is also an increase of precipitation in the storm tracks and in the Arctic during winter but again most pronounced in the GHG experiment. In the tropics outside the equatorial zone there is a general reduction in precipitation, indicating a tendency to an enhancement of the meridional circulation (and stronger subsidence outside the ITCZ) associated with a stronger Hadley circulation.

6. Concluding remarks

We have given here a broad account of recent studies of the hydrological cycle mostly undertaken at the Max Planck Institute for Meteorology in Hamburg. It is found that high resolution numerical models are increasingly improving the capability to simulate precipitation at least at middle and high latitudes and where we have the capability to verify the result. The GEWEX subprograms will here play an important role. It seems that in an area like the Baltic Sea and its catchment region we should be able to reproduce the hydrological cycle with considerable accuracy. For an accurate reproduction of global precipitation we are very much hampered by not knowing the global radiation balance at the ground accurately enough. So far we probably only know this with an accuracy of some 10-15 Wm^{-2}, equivalent to some 150 mm/year in evaporation and precipitation.

Climate models have already demonstrated an excellent ability to reproduce precipitation anomalies in relation to the ENSO phenomenon. Recent studies of decadal variations in precipitation as for example observed in the catchment area of the Caspian Sea are promising but more experiments are needed to demonstrate any potential predictability. Present coupled models, though have reached a state of sophistication where such experiments are becoming feasible.

Whether the hydrological cycle will change in a future climate and how much it will change is still difficult to know. Model experiments with increased greenhouse gases only show an overall increase, in particular over land and at high latitudes specially in winter. When the effect from aerosols is considered the answer is less clear, and as has been shown in the experiment we have reported here, there may even be a reduction in the hydrological cycle. More experimentation with different models and by means of ensemble prediction is certainly required to obtain a better understanding of this important problem.

Acknowledgment

I have here drawn on results from experiments carried out at the Max Planck Institute for Meteorology. I am particularly grateful to K. Arpe, S. Bauer, D. Jacob, E. Roeckner and M. Stendel. Many of the results shown here are from studies undertaken by them. I also wish to acknowledge the technical assistance by M. Esch, K Müller, K. Niedl and N. Noreiks.

References

Arkin, P.A. and B.M. Meisner, 1987: The relationship between large-scale convective rainfall and cold cloud over the western hemisphere during 1982-1984. Mon. Wea. Rev., **115**, 51-74.

Arpe, K., L. Bengtsson, A. Eliseev, G. Golitsyn, V. Meleshko, A. Mescherskaya, I. Mokhov, V. Semenov and P. Sporyshev, 1998: Water cycle variability in the Caspian Sea basin. Observations and model results (In preparation).

Baumgartner, A. and E. Reichel, 1975: The world water balance. Elsevier, New York.

Bengtsson, L., 1995: On the simulation and validation of the hydrological cycle in the climate system. Modern Dynamical Meteorology, Proceedings from a Symposium in Honour of Aksel Wiin-Nielsen, Ed. P. Ditlevsen (ECMWF press), 49-68.

Bengtsson, L., S. Bergström, G. Elgered, D. Eppel, C. Fortelius, B. Hansen-Sass, D. Jacob, M. Hantel, A. Lehmann, E. Ruprecht and R. Smith, 1997: Progress report for NEWBALTIC (Contract No. ENV4-CT95-0072). Hamburg, April 1997, pp. 93.

Bergeron, T., 1970: Mesometeorological studies of precipitation, IV. Orogenic and Convective Rainfall Patterns. Report No. 20, Department of Meteorology, Uppsala, Sweden.

Bromwich, D.H., 1990: Estimates of Antarctica precipitation. Nature, **343**, 627-629.

Chahine, M., 1992: The hydrological cycle and its influence on climate. Nature **359**, 373-380.

Gibson, J.K., P. Kallberg, S. Uppala, A. Hernandez, A. Nomura and E. Serrano, 1997: ECMWF Re-analysis Project Report Series: 1. ERA description. Available from ECMWF, 71pp.

Golitsyn, G.S., 1995: The Caspian Sea level as a problem of diagnosis and prognosis of the regional climate change. Izvestiya, Atm. and Ocean. Phys., **31**, No. 3.

Grody, N.C., 1991: Classification of snow cover and precipitation using the Special Sensor Microwave Imager (SSM/I). J. Geophys. Res., **96**, 7423-7435.

Hagedorn, R., 1998: personal communication.

Jacob, D. and R. Podzun, 1997: Sensitivity Studies with the Regional Climate Model REMO. Metorology and Atmospheric Physics **63**, 119-129.

Jaeger, L., 1976: Monatskarten des Niederschlags für die ganze Erde. Berichte des Deutschen Wetterdienstes, Nr. **139 (18)**, Offenbach a.M., 38 pp.

Janowiak, J.E. and P.A. Arkin, 1991: Rainfall variations in the Tropics during 1986-1989, as estimated from observations of cloud-top temperatures. J. Geophys. Res., **96**, 3359-3373.

Jeuken, A.B.M., P.C. Siegmund, L.C. Heijboer, J. Feichter and L. Bengtsson, 1996: On the potential of assimilating meteorological analyses in a global climate model for the purpose of model validation. J. Geophys. Res., **101**, 16939-16950.

Jung, T., E. Ruprecht and F. Wagner, 1998: Determination of cloud liquid water path over the oceans from SSM/I data using neural networks. J. of Appl. Met. In press.

Krishnamurti, T.N., J. Xue, H.S. Bedi, K. Ingles, D. Oosterhof, 1991: Physical initialization for numerical weather prediction over the Tropics. Tellus, **43AB**, 53-81.

Legates, D.R. and C.J. Willmott, 1990: Mean seasonal and spatial variability in gauge corrected global precipitation. J. Clim., **10**, 111-127.

Ohmura, A. and H. Gilgen, 1993: Re-evaluation of th global energy balance. Geophys. Monogr. **75**, IUGG 15, 93-110.

Ramanathan, V., B. Subasilar, G.J. Zhang, W. Conant, R.D. Cess, J.T. Kiehl, H. Graßl and L. Shi, 1995: Warm pool heat budget and shortwave cloud forcing: A missing physics? Science **267**, 499-503.

Ramanathan, V., 1998: Trace gas greenhouse effect and global warming. Underlying principles and outstanding issues. Submitted for publication in Ambio.

Rodionov, S.N., 1994: Global and regional climate interaction: the Caspian Sea experience. Water Science and Technology Library, **11**, Kluwer Academic Publishers, 241 pp.

Roeckner, E., J.M. Oberhuber, A. Bacher, M. Christoph and I. Kirchner, 1996: ENSO variability and atmospheric response in a global coupled atmosphere-ocean GCM. Climate Dyn., **12**, 737-754.

Roeckner, E. et al., 1998: Climate change simulations with a coupled atmosphere-ocean GCM including the tropospheric sulfur cycle. In preparation.

Rudolf, B., H. Hauschild, W. Rüth and U. Schneider, 1996: Comparison of raingauge analyses, satellite-based precipitation etimates and forecast model results. Adv. Spac Res., **7**, 53-62.

Stendel, M. and K. Arpe, 1997: Evaluation of the hydrolagical cycle in reanalyses and observations. Max-Planck-Institut für Meteorologie, Hamburg, Report No. 228, 52 pp.

Trenberth, K., 1997: Using atmospheric budgets as a constraint on surface fluxes. J. of Clim., **10**, 2796-2809.

Weng, F. and N.C. Grody, 1994: Retrieval of cloud liquid water using the Special Sensor Microwave Imager (SSM/I). J. Geophys. Res., **99**, 25535-25551.

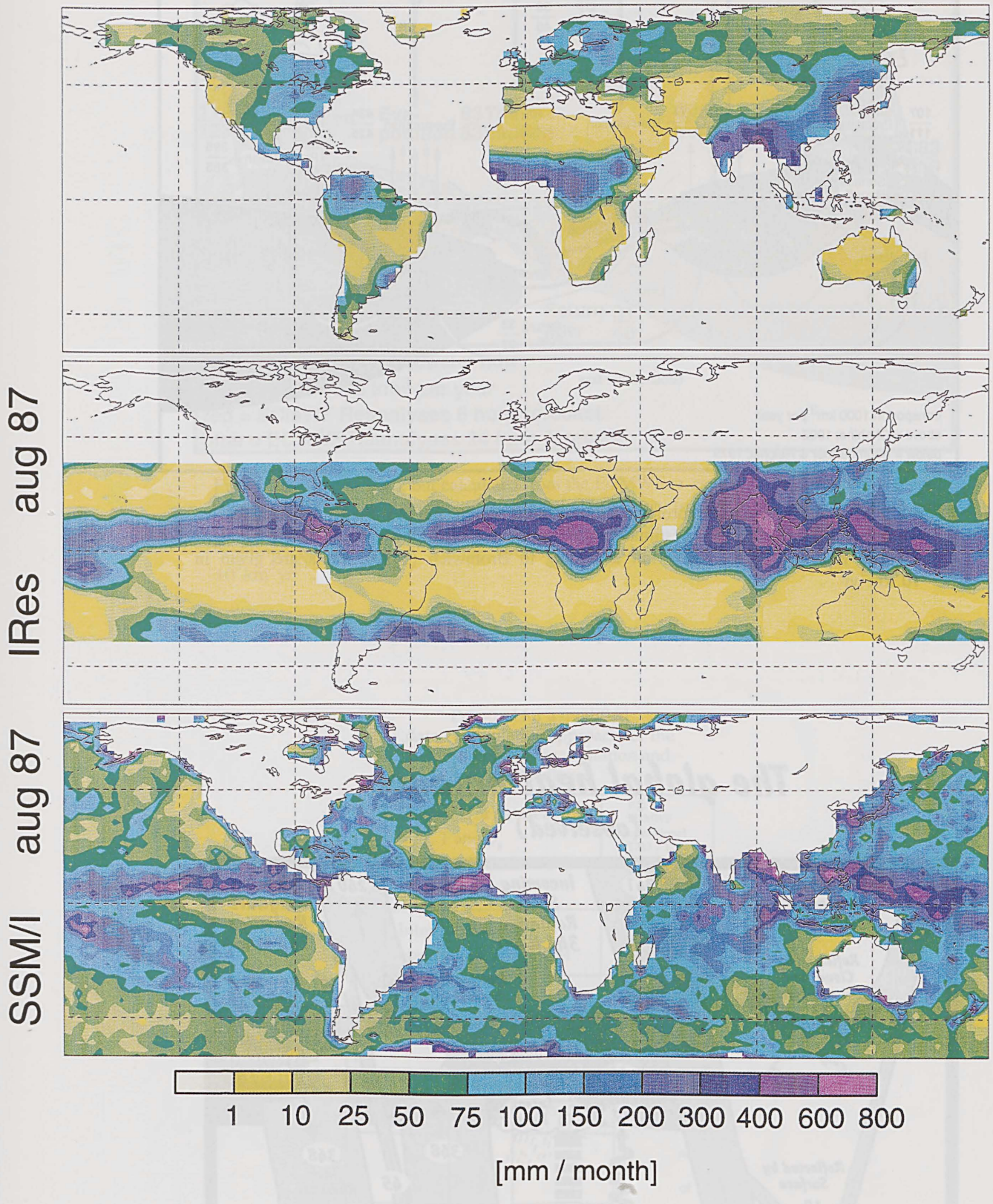

Fig. 1: Three different precipitation estimates for August 1987. Top figure shows measurements from land surface stations, middle figure estimate based on outgoing long wave radiation and the lower figure estimate based on SSM/I data. Although the different estimates are partly confined to different regions the differences are apparent. For further comments see text.

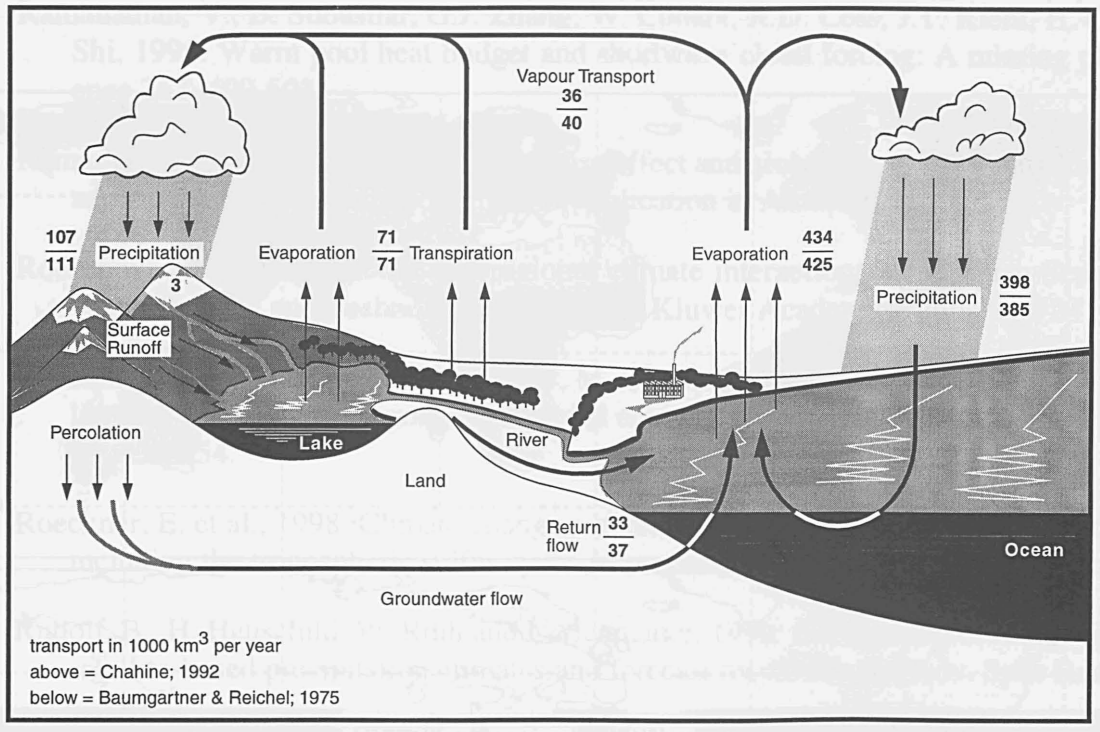

Fig. 2: Global annual mean hydrological cycle for the marine and continental hemispheres, respectively. Upper figure shows estimate from Chahine (1992) and lower figure from Baumgartner and Reichel (1975). Snow fall according to Bromwich (1990). Units are given in $10^3 km^3 yr^{-1}$.

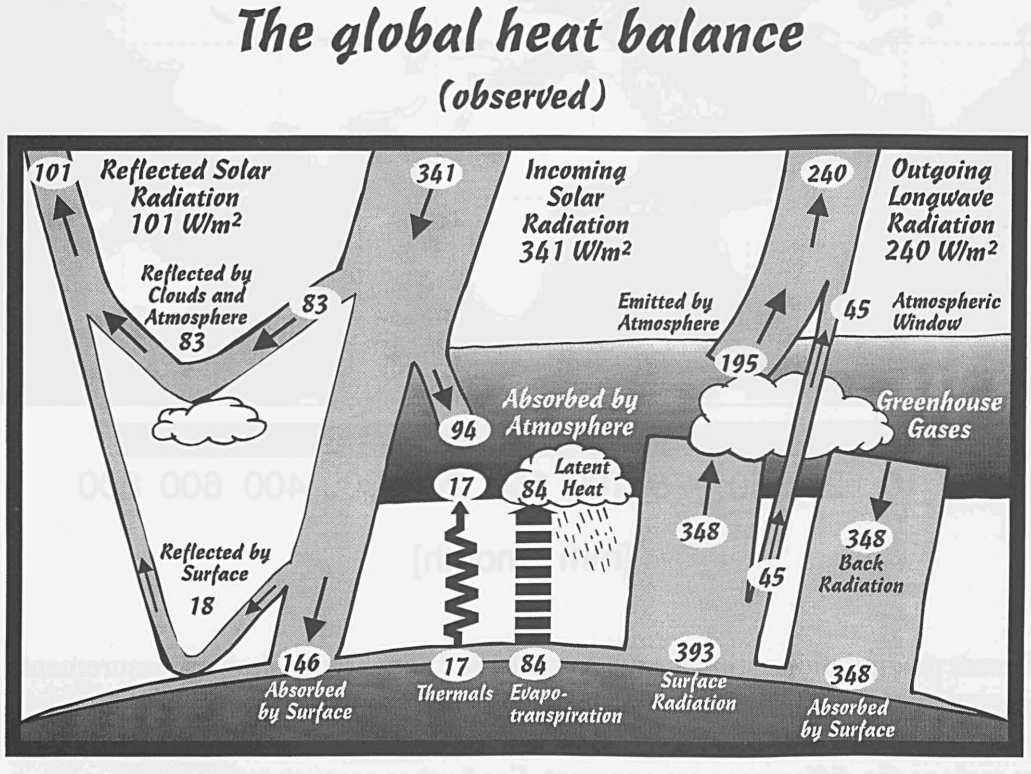

Fig. 3: The global heat balance of the atmosphere, annually averaged. The actual values are compiled from different sources. For further information, see text. Units are in Wm^{-2}.

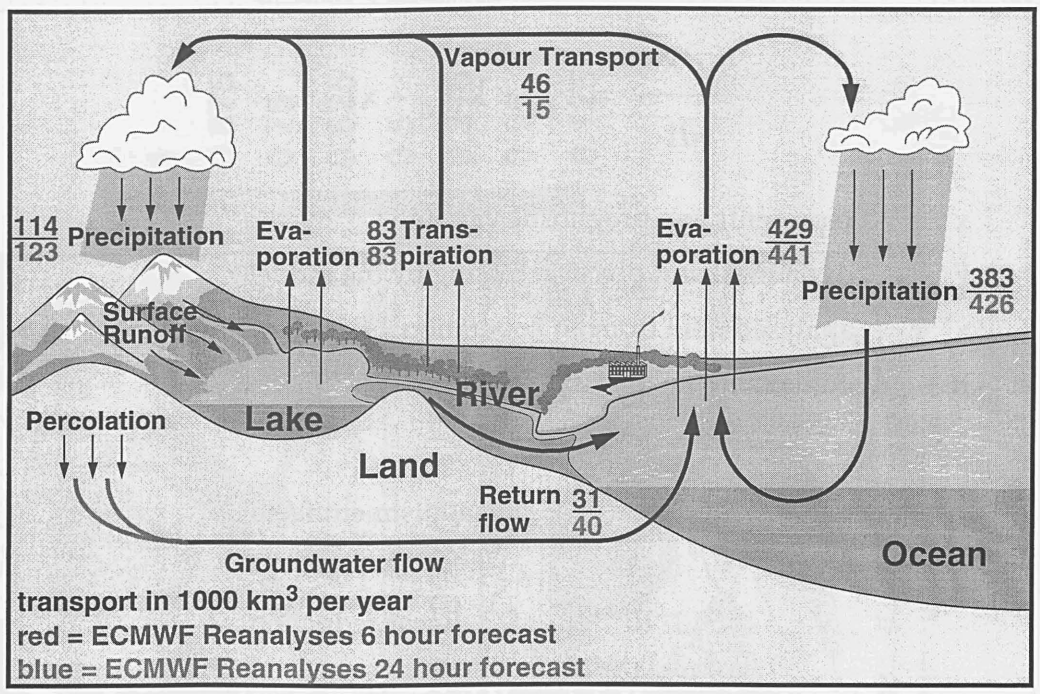

Fig.4: The same as Fig.2 but calculated from the ECMWF re-analysis data, 1979-1993. Upper figures show data calculated from the ensemble of all 6 hour forecasts (first guess) and the lower figure data calculated from an ensemble of 24 hour forecasts. Note the imbalance as well as the "spin-up" or "spin-down" of the hydrological cycle between 6 and 24 hours. Units in $10^3 km^3 yr^{-1}$.

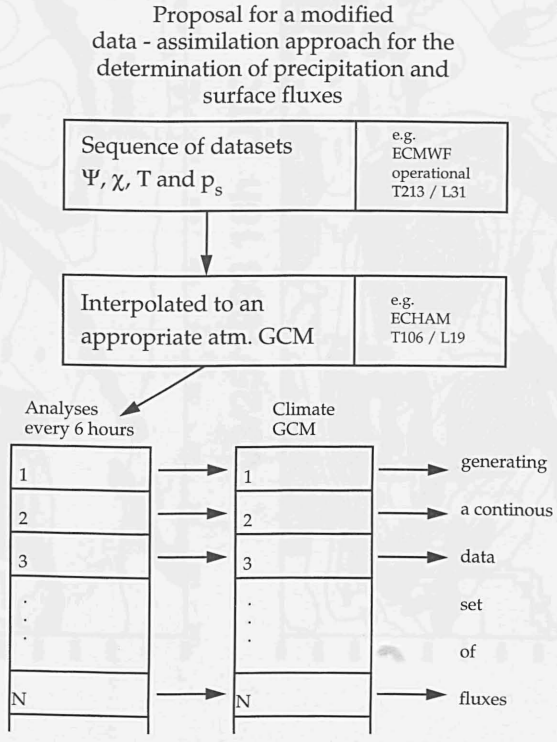

Fig. 5: The diagram shows a modified data-assimilation approach for the determination of precipitation and surface fluxes. The three-dimensional fields of vorticity, divergence and temperature in addition to surface pressure are interpolated to an appropriate GCM at every 6 hours. This new data-set is then used for gradually adjusting the state of the GCM to a sequence of analysed data sets. The actual example shows an interpolation from the ECMWF operational analyses 1993 to the ECHAM GCM at T106 resolution.

$$\frac{\partial x}{\partial t} = F_m + k(x_a - x)$$

x	represents any prognostic variable
F_m	dynamical and physical forcing by the model
x_a	analysed field from an "operational data-ass. model"
k	adjustment factor (nudging term)

parameter	adjustment factor		
	$N \leq 42$	$42 < N \leq 72$	$N > 72$
ψ	$1 \cdot 10^{-4}$	linear reduction	0
χ	$0.5 \cdot 10^{-4}$	-„-	0
T	$1 \cdot 10^{-5}$	-„-	0
p_s	$1 \cdot 10^{-4}$	-„-	0

Fig. 6: The diagram shows the nudging adjustment used in the numerical experiment described in Fig.5.

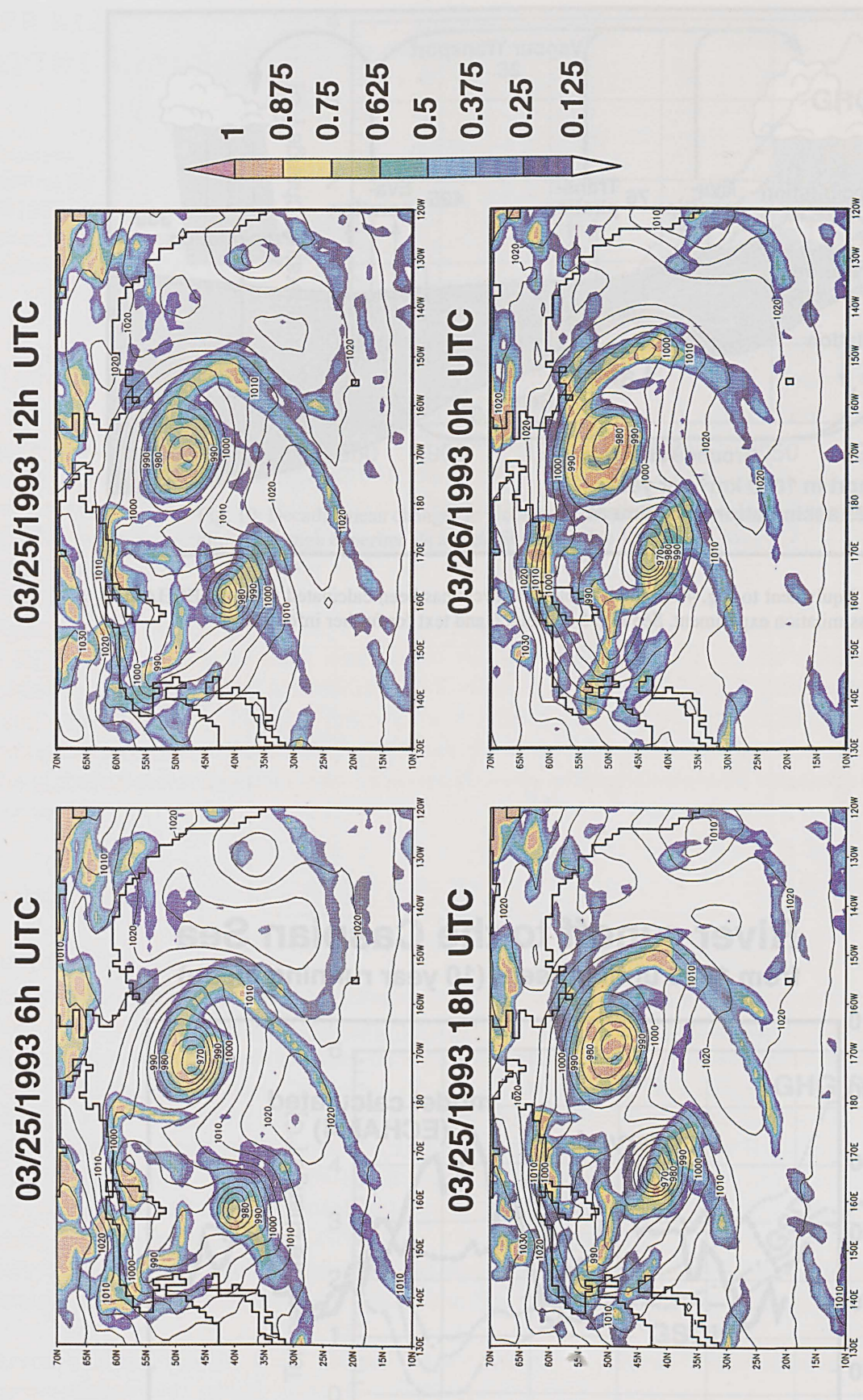

Fig. 7: Mean sea level pressure and cloud fraction at 850 hPa for a time-sequence of fields during 25 March 1993 over the Pacific Ocean. The frontal structure and the occlusion process is clearly indicated. It should be noted that moisture data was not used in this assimilation.

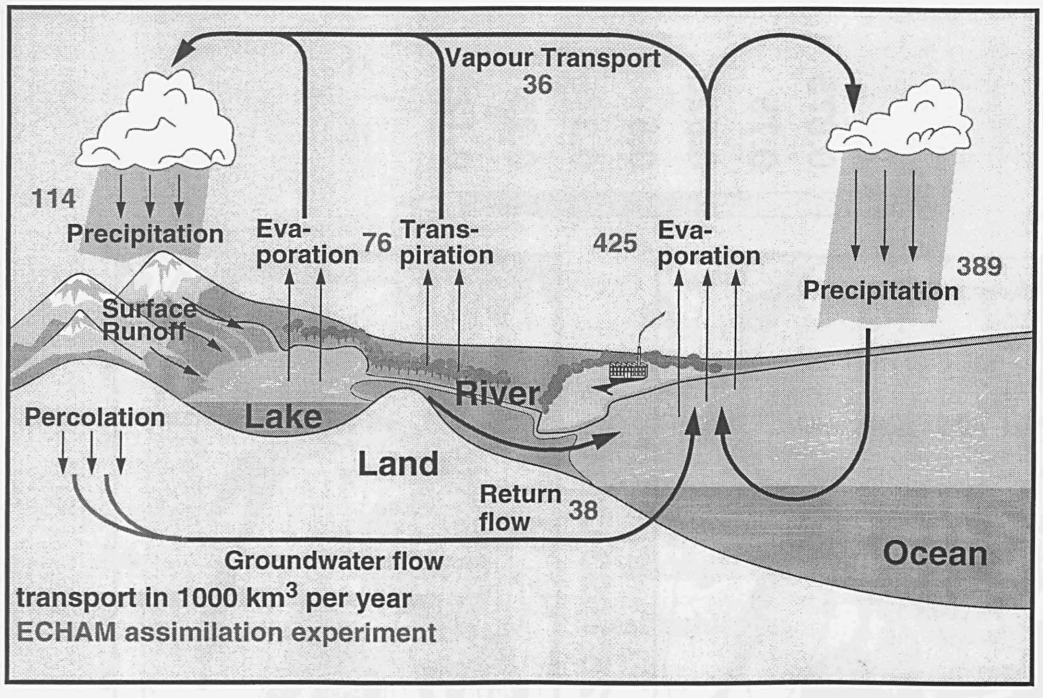

Fig. 8: Equivalent to Fig. 4 but the hydrological cycle has been calculated from the ECHAM data-assimilation experiment. See Fig. 5 and Fig. 6 and text for further information.

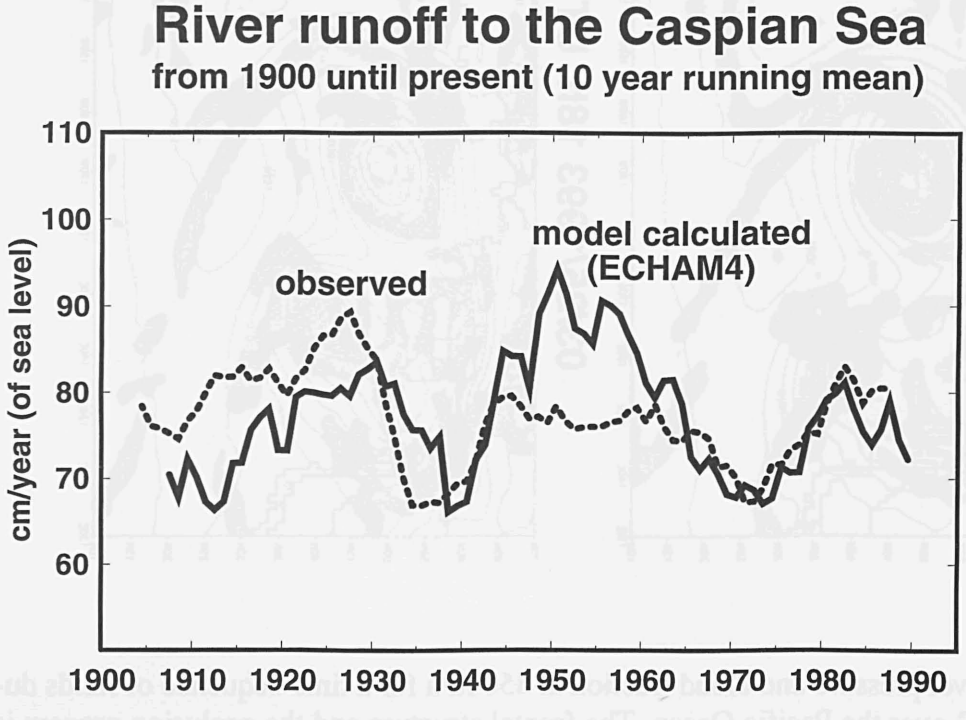

Fig. 9: Observed and model calculated river run-off to the Caspian Sea from 1900-1995 (5-year average). The units are expressed in cm/year of sea level change. The ECHAM4 model has been forced by observed SST data.

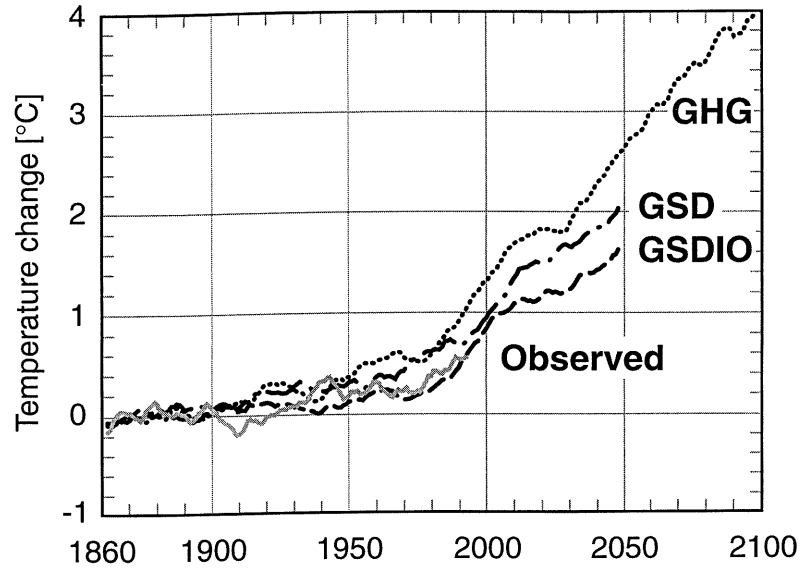

Fig. 10: Decadal mean changes in globally averaged surface temperature (°C) in three different climate change experiments as described in Table 1.

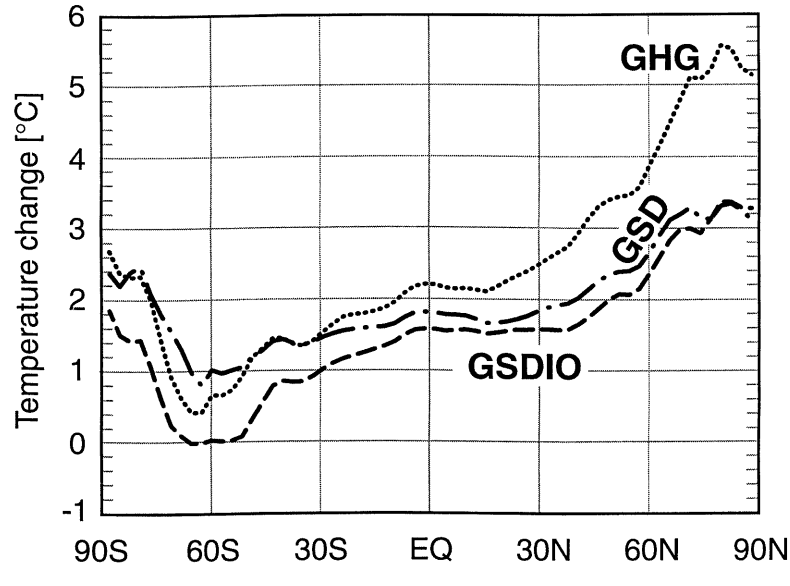

Fig. 11: Temperature changes in the experiments GHG, GSD and GSDIO during the 2040s compared to the control. For further information, see text.

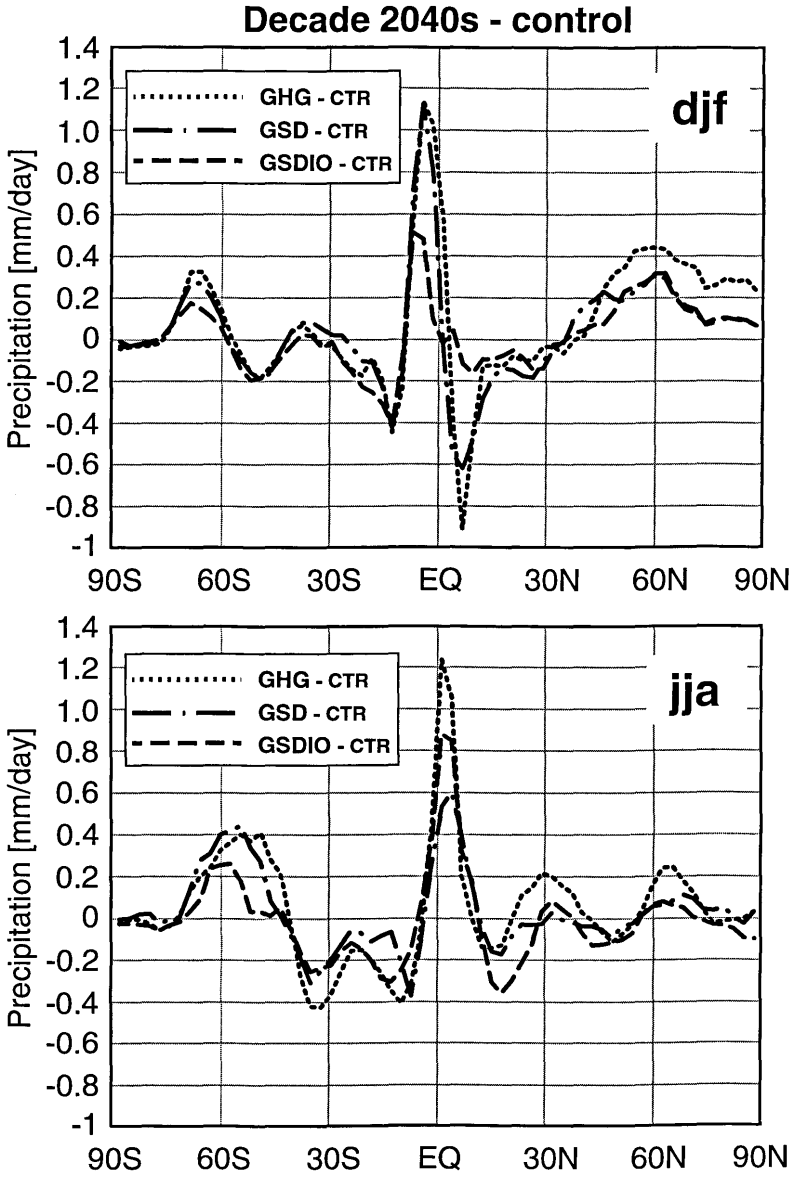

Fig.12: Precipitation changes in the experiments GHG, GSD and GSDIO during the 2040s compared to the control for winter and summer, respectively. Units in mm/day. For further information, see text.